The breakdown of the Stokes–Einstein relation in supercooled binary liquids

2003 J. Phys.: Condens. Matter 15 5397

(http://iopscience.iop.org/0953-8984/15/32/301)

INSTITUTE OF PHYSICS PUBLISHING JOURNAL OF PHYSICS: CONDENSED MATTER

J. Phys.: Condens. Matter **15** (2003) 5397–5407 PII: S0953-8984(03)62918-8

The breakdown of the Stokes–Einstein relation in supercooled binary liquids

Patrice Bordat[1,2], **Frédéric Affouard**[1], **Marc Descamps**[1] **and Florian Müller-Plathe**[2]

[1] Laboratoire de Dynamique et Structure des Matériaux Moléculaires, UMR 8024, Université Lille I, 59655 Villeneuve d'Ascq cedex, France
[2] Max-Planck-Institut für Polymerforschung, Ackermannweg 10, D-55128 Mainz, Germany

E-mail: bordat@cyano.univ-lille1.fr

Received 30 April 2003, in final form 16 June 2003
Published 1 August 2003
Online at stacks.iop.org/JPhysCM/15/5397

Abstract

Using reverse non-equilibrium molecular dynamics simulations, we report the calculation of the shear viscosity and the tracer diffusion coefficient of a binary Lennard-Jones mixture that is known as a model glass-former. Several remarkable temperatures are well reproduced in our calculations, i.e. T_S (the onset of slow dynamics), T_c (the critical temperature predicted by the mode-coupling theory) and T_K (the Kauzmann temperature). A breakdown of the Stokes–Einstein relation is found at temperature T_S. We propose that, at low temperatures below T_S, the size of single-particle positional fluctuations between particle-hopping events corresponds to the length measured by the Stokes–Einstein relation, which is equated to the hydrodynamic radius of particles at high temperatures.

1. Introduction

The elusive nature of glassy systems relates to the sharp rise in the transport coefficients (viscosity or relaxation times) in a narrow temperature range above the calorimetric transition temperature, T_g. Despite great interest in glassy systems over the past 40 years, as revealed by the development of several models and theories [1–5], a complete understanding of the glassy state and glass formation has not yet emerged. Some of the most recent investigations focus on the picosecond–nanosecond timescale, where it is suspected that the onset of features of the glass transition phenomena occur. Some paradigms and precise theories have been developed especially to explain the behaviour of supercooled liquids [5] in this domain and from the point of view of the potential energy landscape. Dynamic processes could be described in this fast regime over a temperature range $T_c < T < T_S$ that involves two characteristic temperatures:

(i) The critical temperature, T_c, predicted by the mode-coupling theory (MCT) [6, 7]. T_c corresponds to an ergodic-to-nonergodic transition in the ideal version of this theory.

It is now commonly considered to be a crossover temperature to a 'landscape-dominated' regime in which diffusion processes can be described in terms of thermally activated jumps.

(ii) A second remarkable temperature, denoted T_S (although T_A or T_x are also seen), whose nature is still unclear at present. T_S is detected above T_c, where non-exponential relaxation and non-Arrhenius behaviour are first observed. This marks the crossover from a normal liquid to slow dynamic behaviour. Both temperatures T_c and T_S have been identified in liquid glass-formers from computer simulations and experiments [8–10], and have also been encountered in many molecular systems [11], in polymers [12] and more recently in protein folding [13].

Diffusion coefficients or shear viscosity are useful parameters for following the evolution of the transport properties of glass-formers from high temperatures (picoseconds–nanoseconds, 10^{-2} Poise) to low temperatures close to T_g (seconds, 10^{12} Poise). Several experimental studies [14–21] have determined the diffusion coefficients and the shear viscosity of systems that have the ability to form a glass, and these works have pointed out the deviation from the Stokes–Einstein relation in the $[T_c, T_S]$ crossover temperature range, below a temperature of about 1.2 times the glass transition temperature. This phenomenon is still not understood and some hypotheses have been suggested, such as the *cage effect* of particles or the existence of dynamic heterogeneities [20–22].

In this work we have performed molecular dynamics simulations of a binary Lennard-Jones mixture in order to clarify the mechanisms responsible for the breakdown of the Stokes–Einstein relation. We have calculated the translational diffusion coefficient and the shear viscosity using a recent technique called reverse non-equilibrium molecular dynamics (RNEMD) [23, 24] which provides faster convergence than the usual numerical methods [25]: i.e. shear flow (non-equilibrium MD) or fluctuations of the stress tensor (equilibrium MD). This RNEMD method is based on the phenomenological relation:

$$J_z(p_x) = -\eta\left(\frac{\partial v_x}{\partial z}\right), \tag{1}$$

where $(\frac{\partial v_x}{\partial z})$ is the shear, $J_z(p_x)$ is the transverse momentum flux, and η is the shear viscosity. This method differs from the usual techniques because $J_z(p_x)$ is *imposed* and the shear is *measured*. In the z direction, the simulation box is divided into N_{slab} slabs. Two slabs, spaced by half the simulation box, move oppositely in the x direction to mimic the shear. This motion is achieved by suitably selecting two particles (one particle in each of these two slabs) and exchanging x components of their velocities. This exchange corresponds to an unphysical momentum transfer. As momentum is conserved, the system responds with a physical flux in the opposite direction. The physical flux leads to a velocity profile. After the two fluxes reach the same magnitude and the system converges towards a steady state, we can calculate the shear viscosity. For details of the RNEMD method, which can be used without an external thermostat, see [24]. This method has also been applied to the calculation of the thermal conductivity [26] and the thermal diffusion coefficient [27, 28] (the Ludwig–Soret effect).

2. Computational details

All simulations were performed with the molecular dynamics package YASP [29], in which the RNEMD method was implemented [24]. We use a binary Lennard-Jones system composed of 1500 particles (1200 of species 1 and 300 of species 2), which has been studied extensively as a model glass-former [30–32]. The particles interact via non-additive Lennard-Jones potentials

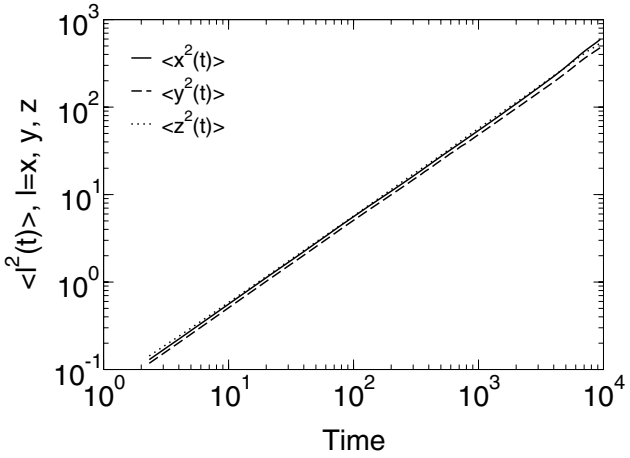

Figure 1. Mean square displacements (MSDs) in the x (solid line), y (dashed line) and z (dotted line) directions of species 1 versus time from a non-equilibrium simulation at $T = 1.66$ with an exchange period of 300 time steps.

Table 1. The parameters of the Lennard-Jones potentials that describe the three types of interactions in the binary mixture.

Interaction	1–1	2–2	1–2
ε	1.0	0.50	1.5
σ	1.0	0.88	0.8

with the parameters collected in table 1, and they are not charged. We use the Lennard-Jones reduced units [33] with σ_1, ε_1 and m_1 as the reference length, energy and mass. A cut-off of 2.9369 is applied. In previous work, Lennard-Jones potentials have been truncated at $r_{\alpha\beta} = 2.5\sigma_{\alpha\beta}$ (with $\alpha, \beta = 1, 2$) and shifted for more efficient molecular dynamics simulations. It can be shown that these truncation details have only a minor influence on the dynamics and the structure of the system. The neighbour list cut-off is 3.23055, and it is updated every 15 time steps. The time step is 2.3218×10^{-3}. The simulations are performed in the NVT (constant number of particles, constant volume and constant temperature) ensemble using a Berendsen thermostat with a coupling time of 0.23218. The temperature ranges from 0.49887 to 8.3145 and we have performed from 2×10^6 to 8×10^6 time steps, depending on the temperature, in order to get a sufficiently long steady state. Below $T = 0.49887$, the shear viscosity becomes very large ($\eta \approx 10^4$ at $T \approx 0.443$) and the steady state cannot be reached in a reasonable computational time. Non-equilibrium simulations in the NVE (constant number of particles, constant volume and constant energy) ensemble as well as NVT and NVE equilibrium simulations have been performed at different temperatures to check the consistency of the diffusion coefficient and of the shear viscosity. The simulation box is orthorhombic and of size $L \times L \times 3L$, where $L = 7.469$ is chosen to yield a density ρ of 1.2. The simulation box is divided into 20 slabs in the z direction, and the period between velocity (v_x) exchanges is 300 time steps, so the system remains in the linear regime for all temperatures investigated. To get good statistics for the velocity gradient and for the momentum flux, the mean flow velocity within each slab, $\langle v_x(z) \rangle$, and the exchanged momentum are output every 10 time steps. The velocity gradient ($\frac{\partial v_x}{\partial z}$) is obtained by a linear least-squares fit to the velocity profile (excluding the exchange slab).

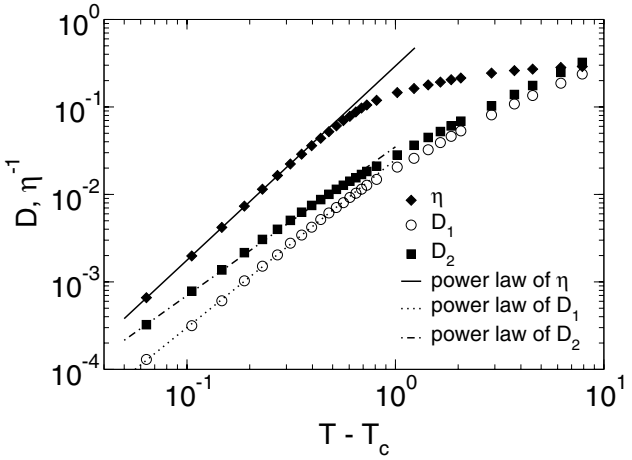

Figure 2. The diffusion coefficient of species 1 (empty circles) and 2 (filled squares), and the inverse shear viscosity (filled diamonds) as a function of the temperature $T - T_c$, where T_c is the critical temperature predicted by the MCT and is fixed at $T_c = 0.435$, according to previous calculations [35]. The lines are power laws of temperature, with exponents of 1.9 (dotted line) and 1.7 (dot–dashed line) for the diffusion coefficients and 2.2 (solid line) for the inverse shear viscosity.

Figure 1 shows the mean square displacements (MSDs) of the x, y and z components obtained from non-equilibrium simulations at $T = 1.66$ with an exchange period of 300 time steps. In this figure, the MSD of the x component is the raw MSD from which a quadratic correction term has been subtracted, which accounts for the part of the displacement in x caused by shearing. This is $V^2_{x,\mathrm{num}}t^2$, where $V^2_{x,\mathrm{num}} = (1/N_{\mathrm{slab}})(\sum_{i=1}^{N_{\mathrm{slab}}}\langle v_{x,i}\rangle^2)$. The quantity $\langle v_{x,i}\rangle$ is an average of the x components of the velocities of all particles within slab i among the N_{slab} slabs and over the time of the simulation once steady state has been reached. Theoretically, the correction could also be obtained from the average velocity in the exchange slab $V^2_{x,\mathrm{theor}} = (2/3L)\int_0^{3L/2}\langle v_x(z)\rangle^2\,\mathrm{d}z = \frac{1}{3}\langle v_{x,1}\rangle^2$ with $\langle v_x(z)\rangle = \langle v_{x,1}\rangle - (4\langle v_{x,1}\rangle/3L)z$. The notations $v_{x,1}$ and $v_x(z)$ refer to the mean velocity of slab 1 (the exchange slab) and the mean velocity at the z coordinate, respectively, due to the shear. The symbol $\langle\cdots\rangle$ represents an average of the simulation over time after steady state has been reached. $V^2_{x,\mathrm{num}}$ and $V^2_{x,\mathrm{theor}}$ are very close; the small difference can be explained by the numerical errors in the velocity profile that make it not rigorously linear. In figure 1, the MSD curves are almost superposed with a slope of 1. This means that the diffusion coefficient in the x, y and z directions are equal, within the error bars. The system is isotropic in diffusion, even though the three directions are not equivalent symmetrically. We have also checked the behaviour of the MSDs in the x, y and z directions for two other exchange periods (100 and 600 time steps) and we have found the same diffusion coefficients. Moreover, we have obtained the same diffusion coefficients, within error bars, by using equilibrium simulations. Thus we conclude that the shear does not affect the single-particle diffusion of the system significantly. The diffusion dynamics are found to be in good agreement with previous studies [34, 35] under equilibrium conditions.

3. Results and discussion

3.1. Determination of outstanding temperatures

Figure 2 shows the diffusion coefficients of both species and the inverse shear viscosity as a function of the temperature $T - T_c$, where $T_c = 0.435$ is the critical temperature predicted

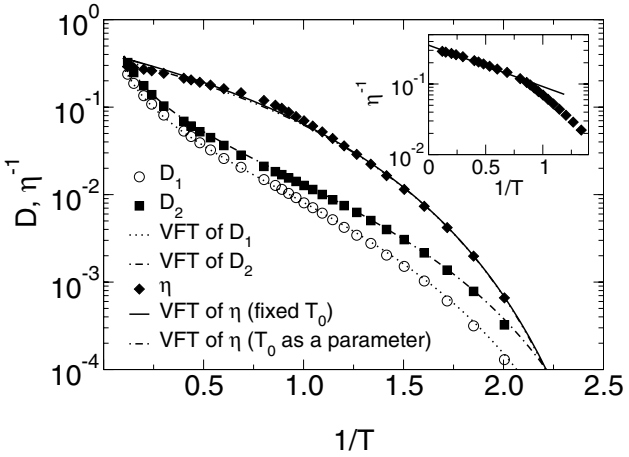

Figure 3. The diffusion coefficient of species 1 (open circles) and 2 (filled squares) and the inverse shear viscosity (filled diamonds) as a function of inverse temperature. The curves for the diffusion coefficients (dotted and dot–dashed curves for species 1 and 2, respectively) correspond to least-squares fits with a modified VFT function (see equation (3)). For the shear viscosity, the curves correspond to VFT functions (see equation (2)), where the limiting temperature T_0 is a parameter (dot–dot–dashed curve) or is fixed to the Kauzmann temperature T_K (solid curve). The inset shows the inverse shear viscosity as a function of inverse temperature and its corresponding Arrhenius fit as a solid curve.

by MCT and previously determined in [35]. The diffusion coefficients exhibit a power-law dependence $(T - T_c)^\gamma$ in a small temperature range above T_c, as predicted by MCT. The exponents—$\gamma \simeq 1.9$ and 1.7 for species 1 and 2, respectively—are found to be in good agreement with previous MD simulations [34, 35]. Above $T = T_S \simeq 1$, the evolution of the diffusion coefficients clearly deviates from the MCT behaviour. It should be noted that Sastry *et al* [9] have associated this change with the onset of slow dynamics, where the system is 'landscape-influenced'. Figure 2 also demonstrates that the shear viscosity follows a power law with an exponent of $\gamma \simeq -2.2$ in the same temperature range as that of the diffusion coefficients. This exponent is found to be in fair agreement with the values of $\gamma \simeq -2.6$ and -2.45 obtained by Kob and Andersen [35] and Berthier and Barrat [36], respectively. The origin of the difference could be due to the better power-law fits for Kob and Andersen [35] and Berthier and Barrat [36], as they investigated lower temperatures closer to T_c.

To identify the different dynamic regimes, the diffusion coefficients of both species and the shear viscosity are displayed in an Arrhenius plot in figure 3. At high temperatures, the shear viscosity follows an Arrhenius law with an activation energy of $T_{act} = 1.31$, as shown in the inset of figure 3. At low temperatures ($T < T_S \approx 1$), the evolution of the shear viscosity deviates from this Arrhenius behaviour. To fit the numerical values of the shear viscosity over the whole temperature range that was investigated, we have used a Vogel–Fulcher–Tammann (VFT) expression:

$$\eta = \eta_\infty \exp\left(\frac{AT_0}{T - T_0}\right). \tag{2}$$

This function characterizes the increase of the shear viscosity as the temperature decreases towards a limit that is denoted by T_0. The parameter A often refers to the fragility of the system and η_∞ is the shear viscosity of the liquid at infinite temperature. The product AT_0 is analogous to the activation energy in the Arrhenius law at high temperatures. For the diffusion coefficients,

Table 2. Parameters of the least mean square fits, using a modified VFT function (see equation (3)) for the diffusion coefficients and a VFT function (see equation (2)) for the shear viscosity.

Diffusion coefficients			
Parameter	ξ	A	T_0
Species 1	31.4	3.30	0.292
Species 2	23.5	2.80	0.295
Shear viscosity			
Parameter	η_∞	A	T_0
Fit 1	2.41	4.49	0.293
Fit 2	2.59	4.30	$T_K = 0.2976$ (fixed)

a VFT function—similar to the one used for the shear viscosity—fits the data well. However, we have used a modified VFT function to fit the numerical values over the largest possible temperature range. This modified VFT function is

$$D = \frac{T}{\xi}\exp\left(\frac{-AT_0}{T - T_0}\right), \tag{3}$$

where ξ is a friction parameter.

The fitted parameters are summarized in table 2. Clearly, all data can be described well by the modified VFT law for the diffusion coefficient of both species and a VFT law for the shear viscosity. Reasonable reliability is expected in this fitting process, since the temperature $T_0 \simeq 0.294$ is almost the same for both transport coefficients. Moreover, $T_0 \simeq T_K$ emerges from our calculations, where $T_K = 0.2976$ is the Kauzmann temperature that was determined in previous MD simulations for the same system [5, 37]. Therefore, T_0 can be considered to be a good estimation of the Kauzmann temperature in our calculations, even if it is known that the VFT fits do not work properly at low temperatures. The correct way of determining T_K should be the calculation of the configurational entropy, as shown in [5, 37] and recently proposed by Coluzzi *et al* [38, 39].

3.2. Breakdown of the Stokes–Einstein relation

Two important dynamic quantities—the diffusion coefficient and the shear viscosity—are accessible in our simulations. Consequently, it is possible to check the validity and the breakdown of the Stokes–Einstein relation as temperature changes. The Stokes–Einstein relation is given by

$$d = \frac{k_B T}{3\pi D\eta} = \text{constant} \tag{4}$$

for stick boundary conditions. Figure 4 shows the evolution of the quantity $d = \frac{k_B T}{3\pi D\eta}$ as a function of temperature. Two curves have been plotted that correspond to d_1 and d_2 obtained from the diffusion coefficient of species 1 and 2, respectively. According to the Stokes–Einstein approximation, the constant d is a length that is defined as the hydrodynamic diameter of the particles. For the case of Lennard-Jones particles, the hydrodynamic diameter corresponds to the diameter of the particles defined by σ. Indeed, at high temperatures (for $T > T_S$), $d_1 = 1.02$ and $d_2 = 0.85$ are found, which are in good agreement with the diameters $\sigma_1 = 1$ and $\sigma_2 = 0.88$ for species 1 and 2, respectively (see figure 4). However, the Stokes–Einstein relation does not hold below T_S, since the apparent length d decreases for both species.

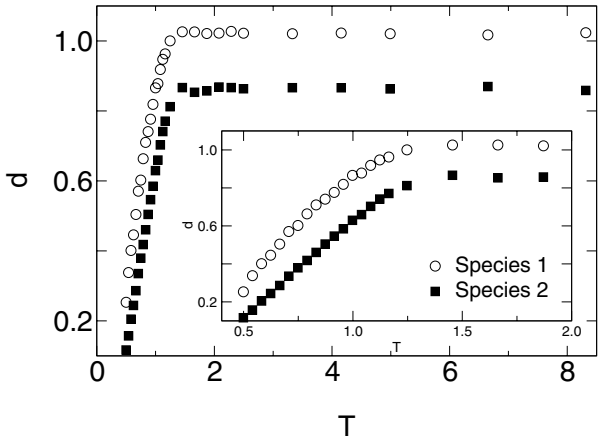

Figure 4. The length d, determined from the Stokes–Einstein relation (see equation (4)) as a function of temperature. Open circles and filled squares are for species 1 and 2, respectively. At high temperatures the length is constant and corresponds to the hydrodynamic diameter of particles. The inset shows length d in the temperature range [0.5–2].

For example, at $T = 0.54$ we find $d_1 = \sigma_1/3.0$ and $d_2 = \sigma_2/5.6$. As the lengths d measured by the Stokes–Einstein relation decrease as temperature decreases, d cannot be associated with a domain size that is expected to grow, lowering the temperature. It should be noted that this behaviour has already been observed in highly viscous silica melt by Horbach and Kob [40] using the appropriate Green–Kubo formula and also by Barrat *et al* [41] for the same model at different pressures and by Yamamoto and Onuki [42] for a binary hard sphere mixture.

Several works have proved that, in the temperature range $[T_c, T_S]$, the continuous diffusion process is replaced by a single-particle hopping process [8, 43–45]. These investigations have shown in particular that particles are confined on sites where they oscillate within a small space for a long time and then hop to another place where they are again localized. This jump corresponds approximately to a particle exchange with near neighbours separated by about σ. This single-particle hopping process has been correlated to the shape of the self-part of the van Hove function [8, 43, 46] and to its non-Gaussian nature [44, 45]. This suggests the existence of clusters of mobile particles. These clusters or groups of particles move faster than the majority of the particles in the system and are therefore called dynamic heterogeneities. In the inset of figure 5 we have plotted the trajectory of a single particle projected on the (y, z) plane at $T = 0.54$. The hopping process can clearly be seen: the trajectory of the particle is localized at three different sites that are highlighted by circles and separated by jumps. The size of the jumps is about σ and the radius of the circles is about $\frac{\sigma}{3}$.

This single-particle hopping process is also revealed in figure 6 by the existence of a subdiffusive regime, i.e. a plateau-like domain in the MSD curves. At low temperatures in the plateau regime the MSD curves can be fitted with the von Schweidler law, which depends on an exponent b in relation to the exponent γ, as predicted in MCT and used in figure 2. We found $b \approx 0.45$, which is in good agreement with the previous estimations of 0.48–0.52 according to Kob and Andersen [47, 48]. The plateau regime is defined between two inflexion points: the first one marks the end of the ballistic regime and the second indicates the start of the diffusive regime. The time dependence of the diffusive regime has been fitted by using a linear law t, whereas a power law t^α ($\alpha < 1$)—inspired by the von Schweidler law—has been used for the subdiffusive regime. A characteristic length, λ, can be derived from the intersection of subdiffusive and diffusive regimes, identified as point A in figure 6. The length λ corresponds

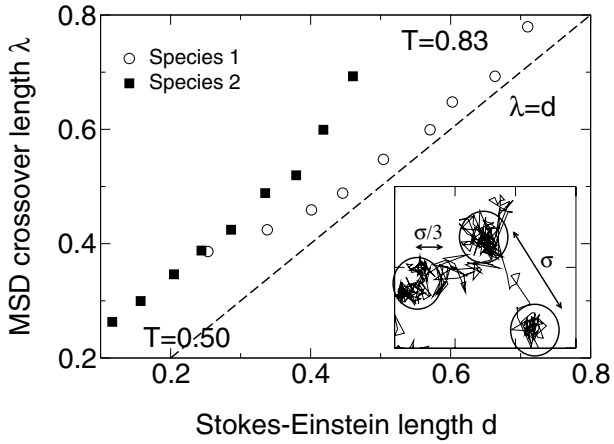

Figure 5. The length λ of the subdiffusive-to-diffusive crossover, determined from the MSD curves, versus the apparent hydrodynamic diameter d from the Stokes–Einstein relation (see equation (4)) for species 1 (open circles) and 2 (filled squares) at different temperatures ($T = 0.5$, 0.54, 0.58, 0.62, 0.66, 0.71, 0.75, 0.79, 0.83). The length λ has been multiplied by $\sqrt{3}$ to take into account the x, y and z directions. The inset shows the trajectory of a single particle projected on the (y, z) plane at $T = 0.54$. Its motion is dominated by hopping due to the cage effect. It is the origin of the plateau or the subdiffusive regime observed in the MSD curves at intermediate times.

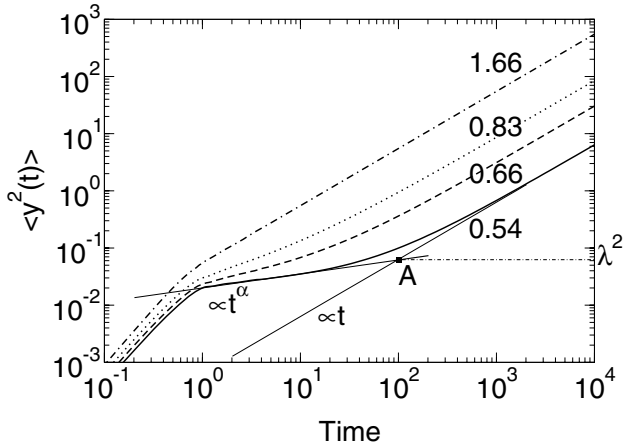

Figure 6. MSD (thick curves) of species 1 along the y coordinate versus time for four different temperatures: $T = 0.54$ (solid), 0.66 (dashed), 0.83 (dotted) and 1.66 (dot–dashed). λ is defined as the ordinate of point A. This point corresponds to the intersection of two fitted lines based on the diffusive regime at long times and on the subdiffusive regime at intermediate times of the MSD. The fitted lines are represented by solid thin lines. This length cannot be defined for $T = 1.66$.

to the distance covered by a particle until the particle succeeds in escaping from the cage formed by its neighbourhood. Therefore, λ provides a measure of the size of the confined regions (cage) explored by the particles. This length (called 'MSD crossover length' in the following) can only be determined if the plateau-like regime is clearly defined. We found $T \simeq T_S$—the highest temperature for which this determination is possible. This confirms the existence of the onset of slow dynamics, as already highlighted by the diffusion coefficient and the shear viscosity. According to the Kob–Andersen model [35], it should be noted

that λ does not converge to zero but to a finite value equal to $r_c\sqrt{(6)} \approx 0.17$, where r_c is the Lindemann localization length. Below T_S, $1/\lambda$ can be considered to be a coupling term between the particle and its neighbours. Indeed, at high temperatures (above T_S) the particles normally diffuse, because they are controlled mainly by their kinetic energy rather than their potential energy. Nevertheless, at low temperatures (below T_S) the intermolecular potential is large compared to the kinetic energy. Thus, the dynamics of the particle are slowed down by the cage effect. This picture is analogous to the 'landscape-influenced' regime proposed by Sastry [9].

In figure 5 we have plotted the MSD crossover length λ versus the apparent hydrodynamic diameter d from the Stokes–Einstein relation at different temperatures between $T = 0.50$ and 0.83. For species 1 we show that $\lambda \approx d$ holds well, which means that the Stokes–Einstein relation is sensitive to the confined fluctuations of the particles. Then the length d extracted from the Stokes–Einstein relation does not correspond to the hydrodynamic diameter σ in the [0.5; 0.83] temperature range. At high temperatures the motion of the particles is governed by the diffusion process. Then the particles move freely to the location of their nearest neighbours, so the positional fluctuations are equal to the hydrodynamic diameter. In this case, jumps and fluctuations become indistinguishable. Yet, at lower temperatures the spatial fluctuations and the jumps (or the hydrodynamic diameter) become uncorrelated. As the Stokes–Einstein relation measures the positional fluctuations and not the jumps, the length d measured by the Stokes–Einstein relation must decrease with temperature. At this stage, this new look at the length d measured by the Stokes–Einstein relation is not incompatible with the hydrodynamic diameter; it is a generalization. As for species 2, λ is described well by a linear function of d, but $\lambda = d$ is not granted. One explanation could be the following. As the system is composed of 1200 particles of species 1 and 300 particles of species 2, one particle of species 2 is more likely to be surrounded by particles of species 1. Therefore, the size of the fluctuations of one particle of species 2 results from the interaction between species 1 and 2 rather than between species 2 and itself. Moreover, as the strength of the potential (ε) of species 2 is only 0.5 compared with 1.0 for species 1 and 1.5 for mixed interactions, the particles of species 1 can overlap the particles of species 2 more: the particles of species 2 can be seen as spheres that are less hard than the particles of species 1. These two observations lead to the diameter d being too small, as measured by the Stokes–Einstein relation. Another point is that the species 2 particles are more mobile than the species 1 particles, so there is greater uncertainty in the fit of the plateau of species 2 and the λ of species 2 is less accurate. It should also be mentioned that, at low temperatures approaching T_c, it is difficult to estimate accurately the diffusion coefficients and the shear viscosity due to the very long relaxation time of the system. Consequently, a relatively large error can be suspected for d.

4. Conclusion

In this paper, we have shown that the RNEMD is a well adapted method for investigating the transport properties of glass-forming systems. RNEMD is a recent technique that provides faster convergence than the usual numerical non-equilibrium or equilibrium methods. A binary Lennard-Jones mixture has been studied that is well documented in the literature and is known as a model glass-former. Despite the very slow dynamics occurring at low temperature, the shear viscosity has been calculated and its temperature dependence has been analysed with other transport coefficients as the diffusion coefficients. Using different fitting laws, we were able to reproduce—with good precision—some outstanding temperatures: i.e. the Kauzmann temperature $T_K \simeq 0.29$ [31], the critical temperature $T_c \simeq 0.435$ [35], predicted by MCT; and the crossover temperature $T_S \simeq 1$ [9], showing the onset of slow dynamics.

From the shear viscosity and the diffusion coefficients of both species, we have calculated the apparent hydrodynamic diameter d from the Stokes–Einstein relation. A temperature-independent constant with an Arrhenius behaviour is found at high temperatures in the normal liquid state, as expected according to hydrodynamics theory. Below T_S, the Stokes–Einstein relation breaks down, as observed in some experiments on glass-former systems. We have shown that the motion of the particles is not described by continuous diffusion but by hoppings between sites where particles are localized. We have correlated the length d, extracted from the Stokes–Einstein relation, with the length λ corresponding to the size of the positional fluctuations of particles on sites where they are localized. This interpretation of the Stokes–Einstein relation is an extension to the original concept and could be useful in understanding the mechanisms of the formation of the glassy state. The breakdown of the Stokes–Einstein relation appears to be a sensitive probe of the jump process when the system starts being 'landscape-influenced'. As the diffusion process also involves the motion of particles over a distance approximately equal to the hydrodynamic diameter at low temperatures, the breakdown of the Stokes–Einstein relation means that the momentum transport described by the viscosity is characterized by another length, which appears in this work as the size of the single-particle positional fluctuations between particle hopping events. This suggestion will be studied in future work.

References

[1] Kauzmann W 1948 *Chem. Rev.* **43** 219
[2] Gibbs J H and DiMarzio E A 1958 *J. Chem. Phys.* **28** 373
[3] Anderson P W 1995 *Science* **267** 1615
[4] Stillinger F H 1988 *J. Chem. Phys.* **88** 7818
[5] Debenedetti P G and Stillinger F H 2001 *Nature* **410** 259
[6] Götze W 1990 *Liquids Freezing and the Glass Transition* ed J P Hansen, D Levesque and J Zinn-Justin (Amsterdam: North-Holland)
[7] Götze W and Sjögren L 1992 *Rep. Prog. Phys.* **55** 241
[8] Schroder T B, Sastry S, Dyre J C and Glotzer S C 2000 *J. Chem. Phys.* **112** 9834
[9] Sastry S, Debenedetti P G and Stillinger F H 1998 *Nature* **393** 554
[10] Richter D and Angell C A 1998 *J. Chem. Phys.* **108** 9016
[11] Kiebel M *et al* 1992 *Phys. Rev.* B **45** 18
[12] Richter D, Frick B and Farago B 1988 *Phys. Rev. Lett.* **61** 2465
[13] Angell C A 1995 *Science* **267** 1924
[14] Ehlich D and Sillescu H 1990 *Macromolecules* **23** 1600
[15] Blackburn F R, Cicerone M T, Hietpas G, Wagner P A and Ediger M D 1994 *J. Non-Cryst. Solids* **172–174** 256
[16] Rössler G and Sokolov A P 1996 *Chem. Geol.* **128** 143
[17] Heuberger G and Silescu H 1996 *J. Phys. Chem.* **100** 15255
[18] Chang I and Sillescu H 1997 *J. Phys. Chem.* B **101** 8794
[19] Ediger M D 1998 *J. Non-Cryst. Solids* **235–237** 10
[20] Chang I, Fujara F, Geil B, Heuberger G and Silescu H 1994 *J. Non-Cryst. Solids* **172–174** 248
[21] Cicerone M T, Blackburn F R and Ediger M D 1995 *J. Chem. Phys.* **102** 471
[22] Ediger M D 2000 *Annu. Rev. Phys. Chem.* **51** 99
[23] Müller-Plathe F 1999 *Phys. Rev.* E **59** 4894
[24] Bordat P and Müller-Plathe F 2002 *J. Chem. Phys.* **116** 3362
[25] Evans D J and Morriss G P 1990 *Statistical Mechanics of Nonequilibrium Liquids* ed D P Craig and R McWeeny (London: Academic)
[26] Müller-Plathe F 1997 *J. Chem. Phys.* **106** 6082
[27] Reith D and Müller-Plathe F 2000 *J. Chem. Phys.* **112** 2436
[28] Bordat P, Reith D and Müller-Plathe F 2001 *J. Chem. Phys.* **115** 8978
[29] Müller-Plathe F 1993 *Comput. Phys. Commun.* **78** 77
[30] Kob W, Donati C, Plimpton S J, Poole P H and Glotzer S C 1997 *Phys. Rev. Lett.* **79** 2827
[31] Sastry S 2000 *Phys. Rev. Lett.* **85** 590

[32] Sciortino F, Kob W and Tartaglia P 1999 *Phys. Rev. Lett.* **83** 3214
[33] Allen M P and Tildesley D J (ed) 1987 *Computer Simulation of Liquids* (Oxford: Oxford Science)
[34] Fourkas J, Kivelson D, Mohanty U and Nelson K (ed) 1997 *Experimental and Theoretical Approaches to Supercooled Liquids: Advances and Novel Applications* (Washington, DC: American Chemical Society)
[35] Kob W and Andersen H C 1995 *Phys. Rev.* E **51** 4626
[36] Berthier L and Barrat J L 2002 *J. Chem. Phys.* **116** 6228
[37] Sastry S 2001 *Nature* **409** 164
[38] Coluzzi B, Parisi G and Verrocchio P 2000 *Phys. Rev. Lett.* **84** 306
[39] Coluzzi B and Verrocchio P 2002 *J. Chem. Phys.* **116** 3789
[40] Horbach J and Kob W 1999 *Phys. Rev.* B **60** 3169
[41] Barrat J L, Badro J and Gillet P 1997 *Mol. Simul.* **20** 17
[42] Yamamoto R and Onuki A 1998 *Phys. Rev.* E **58** 3515
[43] Schroder T B and Dyre J C 1998 *J. Non-Cryst. Solids* **235–237** 331
[44] Weeks E R, Crocker J C, Levitt A C, Schofield A and Weitz D A 2000 *Science* **287** 627
[45] Kegel W K and van Blaaderen A 2000 *Science* **287** 290
[46] Roux J N, Barrat J L and Hansen J P 1989 *J. Phys.: Condens. Matter* **1** 7171
[47] Kob W and Andersen H C 1994 *Phys. Rev. Lett.* **73** 1376
[48] Kob W and Andersen H C 1994 *Nuovo Cimento* D **16** 1291